

# Theoretical Study of Structural and Optical Properties of Noble Metal Cluster-Dipeptide Hybrids at Defect Centers of MgO

Alexander Kulesza,<sup>a</sup> Roland Mitrić,<sup>\*a</sup> and Vlasta Bonačić-Koutecký<sup>\*,b,c</sup>

Received Xth XXXXXXXXXXXX 20XX, Accepted Xth XXXXXXXXXXXX 20XX

First published on the web Xth XXXXXXXXXXXX 200X

DOI: 10.1039/b000000x

We present the theoretical investigation of structural and optical properties of silver and gold cluster-dipeptide hybrids bound to the F<sub>S</sub> defect of the MgO (100) surface. We use DFT and its TDDFT variant combined with the polarizable embedded cluster model for the description of the extended MgO environment. As model peptide we have chosen CysTrp since the cysteine residue interacts strongly with metal particles through the sulphur atom and tryptophan is the most important chromophoric amino acid. Our results show that in the case of CysTrp bound to the supported Ag<sub>4</sub> cluster an intense optical signal arises at 400 nm. In contrast, in the case of gold no strongly localized absorption is present since the optical response of supported gold-peptide hybrids is dominated by a large number of low intensity d-electron excitations spread over a broad energy range. Such localized optical signal which is present in supported silver hybrids can be exploited for the optical detection of peptides and thus can serve as basis for the development of biosensing materials.

## 1 Introduction

One of the most flourishing fields in nanobiotechnology<sup>1–4</sup> involves the development of nanomaterials that combine the recognition and catalytic properties of biomolecules with the unique electronic and optical properties of metallic nanoparticles. In particular, remarkable enhancement of photoabsorption and emission of chromophores, that takes place due to the plasmonic effect of metallic nanoparticles, has been widely recognized<sup>5,6</sup>. Since fluorescence labelling has become one of the central technologies in biosensing, metal particle enhanced fluorescence is of particular importance. Up to now the detection is mostly accomplished using organic fluorophores that can specifically label biomolecules<sup>7,8</sup>. However, such labelling compounds can be avoided if the intrinsic fluorescence of the biomolecule can be enhanced to such extent that sensitivity of detection drastically increases<sup>9,10</sup>. This can be achieved by metallic nanoparticles and therefore the label-free detection became of high interest in a number of applications<sup>11</sup>.

Surface plasmon resonance (SPR) using thin metal films of gold<sup>12</sup> or silver<sup>13</sup> is the most widely used detection tech-

nique. However, in general, optical detection sensitivity is strongly dependent on the size and shape of the nanoparticle<sup>14,15</sup>. The question which arises in the context of the label-free detection concerns the proper choice of metal particles which should strongly localize the enhancement of the optical absorption and emission<sup>16</sup> and at the same time remain biocompatible<sup>17–19</sup>.

Small silver clusters in the size regime where "each atom counts" are ideal candidates for label free detection since they can replace organic dyes as chromophores due to their uniquely strong absorption and emission in the visible and UV range<sup>20–23</sup>. Moreover, it has been shown that small silver clusters in hybrid systems involving biomolecules such as peptides significantly extend and enhance their optical absorption<sup>24</sup>. Also a number of successful applications of small silver clusters in cell imaging<sup>17–19</sup> and single molecule spectroscopy<sup>25</sup> has been reported. Gold clusters show also interesting emissive properties that are governed by large contributions of d-electrons due to the pronounced relativistic effects. Therefore it has been recognized that thiolated and dendrimer-encapsulated gold clusters have high potential in applications of biocompatible fluorophores<sup>26–28</sup>.

From our theoretical investigation of optical properties of noble metal cluster-biochromophore hybrids in the gas phase, the conclusion was drawn that localized enhancement of absorption of biomolecules by silver clusters is unique.<sup>29</sup> This is due to a small density of states in the low energy regime, caused by dominant contribution of s-electron excitations in silver clusters. In contrast, in the case of hybrids with gold clusters the contribution of d-electron excitation is significant

<sup>a</sup> Department of Physics, Free University Berlin, Arnimallee 14, 14195 Berlin, Germany. E-mail: mitric@zedat.fu-berlin.de

<sup>b</sup> Department of Chemistry, Humboldt-Universität zu Berlin, Brook-Taylor-Str. 2, 12489 Berlin Fax: +49 (0)30 2093 - 5573; Tel: +49 (0)30 2093 - 5579; E-mail: vbk@chemie.hu-berlin.de

<sup>c</sup> Interdisciplinary Center for Advanced Sciences and Technology (ICAST), University of Split, Meštrovićevo šetalište bb., 2100 Split, Croatia. Fax: +49 (0)30 2093 - 5573; Tel: +49 (0)30 2093 - 5579; E-mail: vbk@chemie.hu-berlin.de

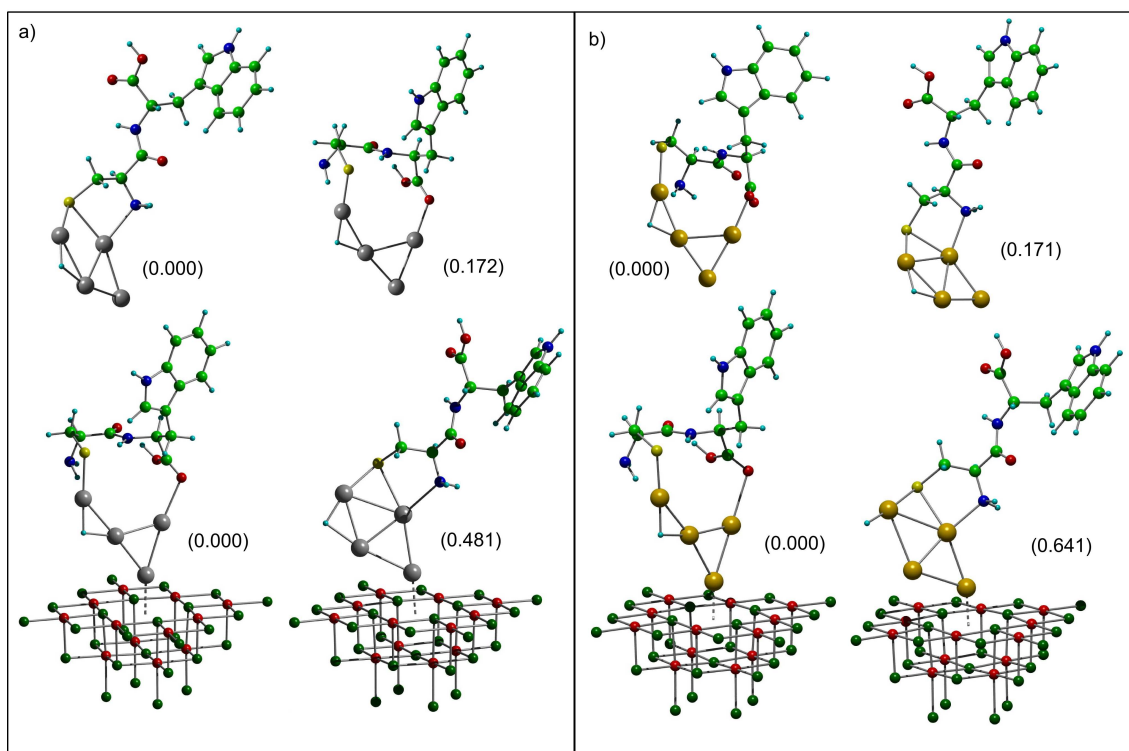


**Fig. 1** Lowest energy isomers for gas-phase and supported a)  $\text{Ag}_4\text{CysTrp}$  and b)  $\text{Au}_4\text{CysTrp}$  hybrid systems. Relative energies in eV are given in brackets.

due to a small s-d energy gap, thus increasing drastically the density of states with low intensities spread in a broad energy interval. These findings may have significant impact for biosensing applications utilizing the metal enhanced fluorescence. However, in the context of proposing new materials, the investigation of optical properties of liganded or supported metal-cluster hybrid systems is mandatory.

Therefore, in this contribution we present a theoretical investigation of the structural and optical properties of silver and gold tetramers interacting with the model dipeptide Cys-Trp and supported at the  $F_S$  defect center of MgO. We have chosen a cystein-containing dipeptide, since typically proteins interact with metal clusters and nanoparticles through the sulphur atom of the Cys residue. Moreover, silver hybrids show unique optical properties due to interactions between excitations within the silver clusters and the indole ring of tryptophan<sup>30</sup>. In addition, our study on structural and optical properties of small noble metal clusters at the  $F_S$ -center defect of the MgO(100) support showed that the smallest clusters are good candidates for emissive centers, since they exhibit long excited state lifetimes<sup>31</sup>. Therefore, our aim here is two-fold. We first show the comparison of optical absorption of the supported hybrid systems involving silver and gold clusters to elucidate the influence of excitations of d-electrons in gold ver-

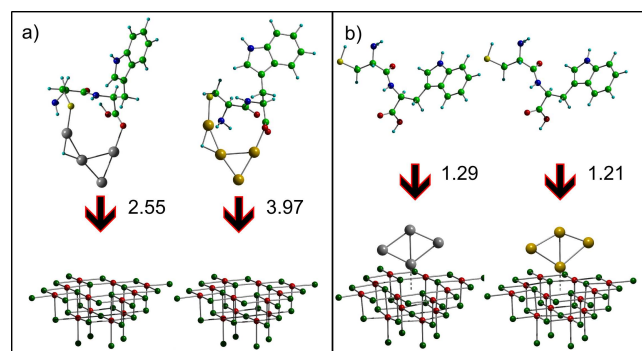


**Fig. 2** a) Binding energies (in eV) of  $\text{Ag}_4\text{CysTrp}$  (left) and  $\text{Au}_4\text{CysTrp}$  (right) to the  $F_S$  defect center of MgO b) binding energies of the CysTrp dipeptide to  $\text{Ag}_4$  (left) and  $\text{Au}_4$  (right) clusters bound to the  $F_S$  defect center of MgO

sus s-electron excitations in silver subunits. Second, we wish to show how the support influences the structural and optical properties of these noble metal-dipeptide hybrids in context of possible label-free biosensing applications.

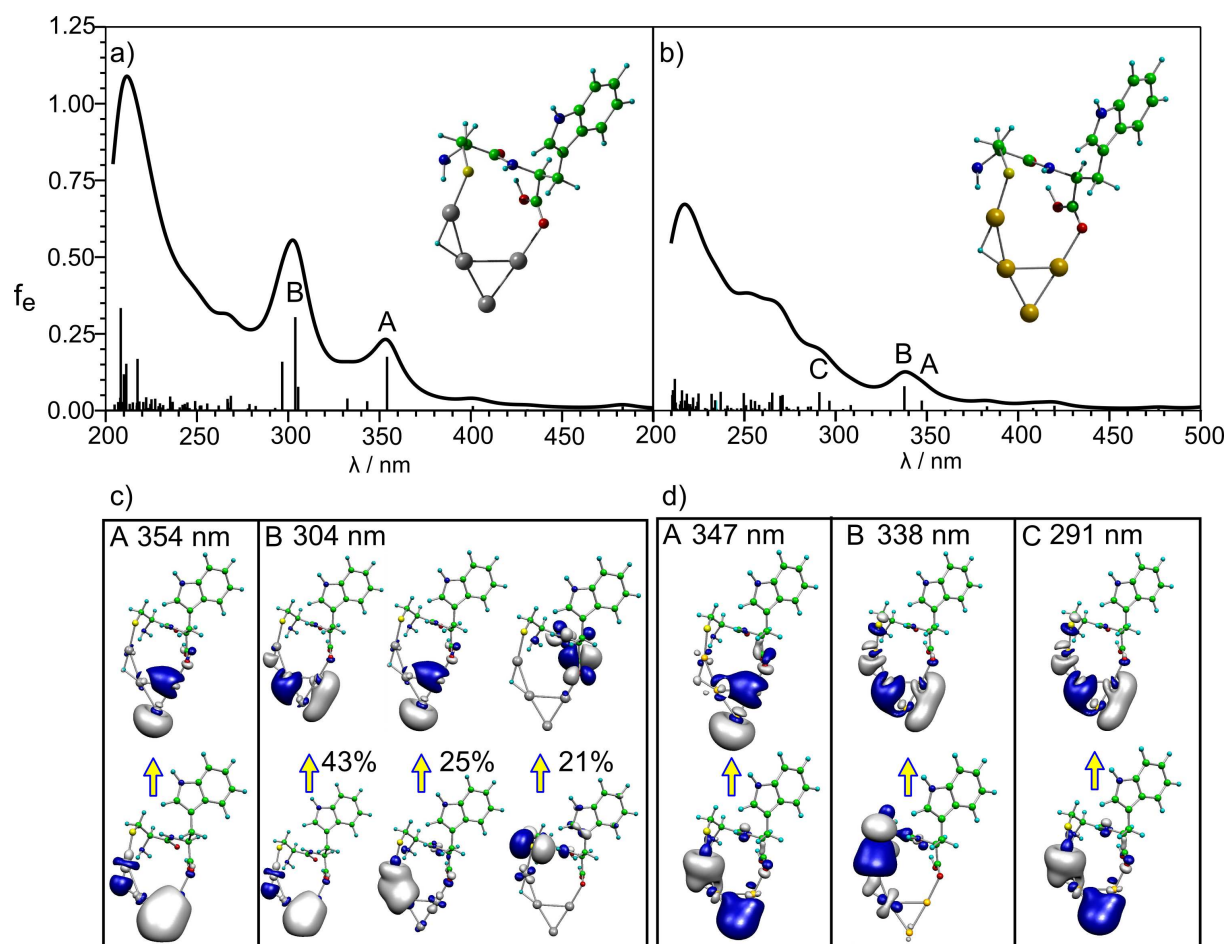


**Fig. 3** a) and b) Calculated absorption spectra for gas-phase  $\text{Ag}_4\text{CysTrp}$  hybrid (left) and  $\text{Au}_4\text{CysTrp}$  hybrid (right) systems. The corresponding structures are shown in the insets. Thermal broadening is simulated by convolution of lines with a Lorentzian function with the half width of 20 nm. c) and d) Analysis of labeled dominant transitions in terms of leading Kohn-Sham orbital excitations for  $\text{Ag}_4\text{CysTrp}$  (left) and  $\text{Au}_4\text{CysTrp}$  (right).

## 2 Computational Methods

Density functional theory (DFT) and its time dependent version (TDDFT) have been used for determination of structural and optical properties of the gas phase hybrid systems, respectively. The same approach was extended for the description of the quantum mechanical part (QM) of the ionic MgO support, as described below.

In order to take into account scalar relativistic effects, 19- $e^-$  relativistic effective core potentials (19- $e^-$  RECP) from the Stuttgart group<sup>32</sup> have been employed for both Ag and Au. For gold the optimized (9s7p5d1f)/[7s5p3d1f] basis set and for all other atoms the triple-zeta plus polarization atomic basis sets (TZVP) have been used<sup>32,33</sup>. Becke's three-parameter non-local exchange functional together with the Lee-Yang-Parr gradient-corrected correlation functional (B3LYP<sup>34-37</sup>)

has been employed to determine structural and optical properties.

An extensive search for structures of the silver hybrid systems was performed using the simulated annealing method coupled to molecular dynamics simulations in the frame of the semiempirical AM1 method<sup>38</sup>. In the case of the gold cluster hybrids the structures of silver cluster hybrid species were used as starting points for searching the lowest energy structures. The vibrational frequencies have been computed in order to find true minima on the potential energy surfaces.

The ionic MgO support was modelled by an embedded cluster approach in which a quantum mechanically (QM) described MgO cluster is embedded into a classical polarizable environment of point charges<sup>39</sup>. The QM part consists of a diamond-shaped  $\text{Mg}_{13}\text{O}_{13}$  section of the MgO (100) surface.  $\text{Mg}^{2+}$  cations are introduced at the boundary of the QM model

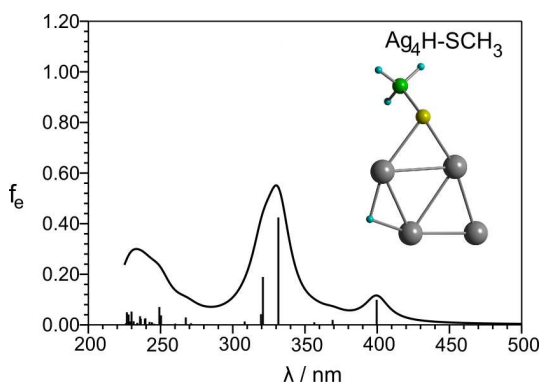


**Fig. 4** Calculated absorption spectrum for  $\text{Ag}_4\text{H-SCH}_3$ , the possible chromophoric subunit present in  $\text{Ag}_4\text{CysTrp}$ . Thermal broadening is simulated by convolution of lines with a Lorentzian function with the half width of 20 nm.

in order to avoid strong polarization by neighboring positive point charges, finally resulting in a  $\text{Mg}_{13}\text{O}_{13}(\text{Mg}^{2+})_{16}$  QM subunit. Removing the central five-fold coordinated surface O atom leads to the creation of the  $F_5$  center defect ( $F_{5c}$ ). The boundary  $\text{Mg}^{2+}$  cations have been described by effective core potentials from Hay and Wadt<sup>40</sup>, replacing the 1s, 2s and 2p electrons, while the valence 3s electrons are described by a single s-AO basis function contracted from two s-type primitive functions.

The QM subunit is embedded in an array of  $20 \times 20 \times 10$  point charges ( $q_{\text{Mg}} = +2.0$ ,  $q_{\text{O}} = -2.0$ ) which simulate the ions of the surrounding lattice ensuring the correct inclusion of the distant part of the electrostatic field of the quasi-infinite crystal (Madelung potential). In order to take into account lattice polarization, these charges are described by the shell model<sup>41</sup>. In this model, an ion is represented by two charges, a point charge core and shell, which are connected by a spring to simulate the dipole polarizability of the environment. They interact between themselves and with the QM subunit ions via specified classical inter-atomic potentials (Coulomb and Buckingham potentials). Corresponding shell model parameters suitable for the MgO surface have been taken from Ref. 42. A small  $10 \times 10 \times 8$  cube of polarizable shell ions (region I) has been chosen to describe the nearest surrounding of the QM subunit in which all point charges (cores and shells) are allowed to relax. The ions outside region I consist of fixed non-polarizable shell ions forming region II.

In order to determine the ground state structural properties of the supported hybrid systems, energetically low-lying isomers obtained for the gas-phase hybrids were placed onto the oxygen vacancy of the  $F_5$ -center with different orientation. Subsequently, full geometry optimization involving hybrid systems, the QM part of the MgO model and shell ions in region I (cores and shells) was performed. For this purpose,

the PBE functional<sup>43,44</sup> has been used together with the Resolution of Identity (RI) approximation<sup>45</sup>, which is adequate for the determination of structural properties and computationally less demanding than using the hybrid B3LYP functional.

All calculations have been performed using the program package TURBOMOLE<sup>46</sup> which allows calculation of energies and forces using analytic gradients acting on QM atoms and point charges for ground as well as excited electronic states<sup>47,48</sup>. An interface program has been developed in order to include the corrections due to the classical environment as well as to provide the interface to the limited-memory Broyden-Fletcher-Goldfarb-Shanno (L-BFGS)<sup>49</sup> optimization routine. The optical properties for optimized structures of supported hybrid systems have been calculated with TDDFT method as for free hybrid systems.

### 3 Results and Discussion

The investigation of structural properties of silver and gold tetramer-Cys-Trp complexes gave rise to the lowest energy class of structures in which one of the metal atoms is inserted into the sulphur-hydrogen bond of cysteine and the other one interacts either with the oxygen atom of tryptophan or with the nitrogen atom of the cysteine as shown in the upper part of Fig. 1. The lowest energy structures of the free silver- and gold-cluster hybrids belong to the latter and the former class of structures, respectively. Both contain  $\text{Ag}_4\text{H}^+$  bound to the thiolate form of cystein ( $\text{R-S}^-$ ). Such metal cluster-hydrogen species were also observed in the gas phase formation of silver clusters using different aminoacids<sup>50,51</sup>. In the case of  $F_5$  center supported hybrids both silver- and gold-cluster complexes interact with atoms belonging to cysteine and to tryptophan as shown in the lower part of Fig. 1. This means that supported silver- and gold-cluster hybrids with CysTrp dipeptide have common structural properties. The binding energy of the gold cluster hybrid system to the MgO  $F_5$  center (see Fig. 2) is considerably stronger than in the case of the silver cluster hybrid due to the larger electron affinity of gold. Moreover, the binding energy of the biomolecule to the supported cluster is lower than the binding energy of the hybrid system to the MgO  $F_5$  center (see Fig. 2), which means that the biomolecule might be reversibly bound and can be removed without destroying the supported cluster. Notice, that the binding energies of CysTrp to the supported  $\text{Ag}_4$  or  $\text{Au}_4$  species (1.29 and 1.21 eV, respectively) are due to the chemical transformation which involves the insertion of the Ag atom into the S-H bond generating a cluster-thiolate species. Therefore it is expected that binding to cystein will be preferred to all other aminoacids.

The TDDFT spectra of free silver- and gold-cluster hybrid systems together with the analysis of leading excitations given in Fig. 3. show clearly, in the case of silver cluster hybrid, that for the intense transition below 350 nm, the excitations

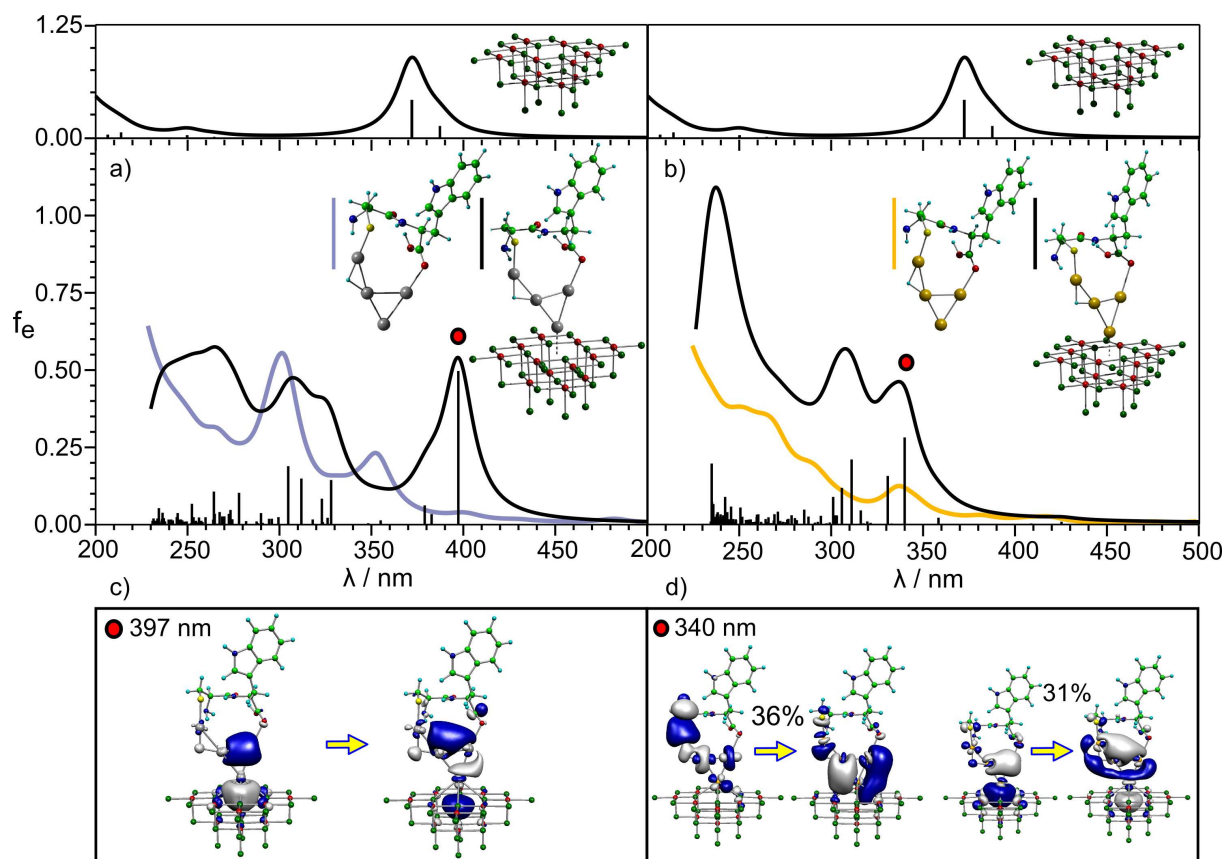


**Fig. 5** Calculated absorption spectra for a) supported  $\text{Ag}_4\text{CysTrp}$  (left) and b) supported  $\text{Au}_4\text{CysTrp}$  hybrid systems. Thermal broadening is simulated by convolution of lines with a Lorentzian function with the half width of 20 nm. For comparison the envelopes of corresponding gas-phase spectra (solid grey and yellow lines) as well as the spectrum of the bare  $F_5$  defect center of MgO (upper panels) are shown. Corresponding structures are also presented in the insets. Analysis of marked dominant transitions in the spectra of supported c)  $\text{Ag}_4\text{CysTrp}$  and d)  $\text{Au}_4\text{CysTrp}$  hybrid systems in terms of leading Kohn-Sham orbital excitations.

are localized within the  $\text{Ag}_3^+$  subunit. This means that the silver subunit is responsible for the low energy spectral properties of the cluster hybrid systems since the transition at 350 nm is not present in the pure CysTrp dipeptide. For the dominant transition around 300 nm the mixture of contributions due to the excitations within the  $\text{Ag}_4\text{H}$  subunit and the charge transfer between the sulphur-bonded part of cysteine and the tryptophan chain is present. This finding is confirmed by the calculated spectrum for the  $\text{Ag}_4\text{H-SCH}_3$  subunit shown in Fig. 4 in which the dominant intense transition is also localized at  $\sim 350$  nm. Due to the electron withdrawing effect by sulphur and oxygen atoms, the  $\text{Ag}_4\text{H-SCH}_3$  model system is characterized by two electrons localized within the  $\text{Ag}_3^+$  subunit. The absorption of  $\text{Ag}_3^+$  is also dominated by intense transition located at 300 nm. In contrast to silver cluster hybrid complex, the spectrum of  $\text{Au}_4\text{CysTrp}$  shown in the right part of Fig. 3 is characterized by high density of transitions with relatively low intensities due to d-electron excitations. Therefore,

the localization of dominantly intense transitions in the lower energy regime is not present as it is the case for silver-cluster hybrid systems.

In order to investigate the influence of  $F_5$  center of MgO support on optical properties of hybrid systems we present the comparison of calculated spectra for  $F_5$  center with those of supported hybrid systems in Fig. 5. The spectra of the free hybrid systems are also inserted in order to discuss qualitatively the outcome of the interaction between hybrid systems with the  $F_5$  center of MgO on spectroscopic fingerprints of supported systems. Since in the case of supported hybrids the  $F_5$  center contributes with two electrons and the dominant transition is located close to 350 nm, in the case of the silver cluster complex the dominant intense transition is shifted to the lower energy of  $\sim 400$  nm. The analysis of this intense transition shows that excitations between the electrons from the  $F_5$  center and the  $\text{Ag}_3^+$  subunit of the hybrid system occur (cf. Fig. 5c). This means that four delocalized valence electrons are

available in the supported system. In fact, the dominant transition of the free  $\text{Ag}_4$  cluster is also localized at 400 nm which is in accord with the above qualitative analysis of the leading features in the spectrum of supported  $\text{Ag}_4$ -CysTrp system. The fundamental quantity relevant for the development of cluster-based biosensors is the change of the optical absorption which occurs upon binding of the biomolecule to the supported cluster. In Fig. 6 we present the difference of the optical spectra between supported  $\text{Ag}_4$ -CysTrp and bare supported  $\text{Ag}_4$ . As can be seen, the binding of the biomolecule causes strong increase of the optical absorption at  $\sim 400$  nm and disappearance of the optical absorption in the visible range at  $\sim 480$  nm. This result indicates that the binding of peptides such as CysTrp can be detected by optical means and thus supported silver clusters can serve as biosensing materials. In contrast, the spectrum for supported gold cluster-hybrid system shown on the right hand side of the Fig. 5 is dominated by the contribution from  $F_5$  center excitations (cf. Fig. 5d) since the transitions for  $\text{Au}_4$ -CysTrp are spread over a large energy interval due to the high density of d-electron excitations.

The above findings clearly show the advantage of supported small silver-hybrid systems which may be good candidates for the development of new nanostructured biosensing materials. Interestingly enough, the combination of the interaction between the subsystems and the number of electrons contributing from the metallic subunit and the electrons from the  $F_5$  center are determining the optical properties of the  $\text{Ag}_4$ -CysTrp hybrid supported system. The above described results can serve as the starting point to guide the design of emissive cluster-hybrid centers stabilized by the support or by the ligands. Supported cluster-hybrid systems can be used to build nanostructured arrays for biochips that are employed for diagnostics of human serum samples, while ligand-protected clusters might serve for sensing in living cells.

## 4 Conclusions

We have presented the theoretical study of the optical properties of silver and gold cluster-peptide hybrid systems supported at the  $F_5$  center defects of the MgO surface. Our results show that the binding of the peptide to the supported silver cluster leads to the appearance of the strong absorption at 400 nm which can be used as an optical signal for the detection of peptides. The strong localized absorption arises due to excitations of delocalized electrons in the  $\text{Ag}_3^+$  structural subunit combined with the  $F_5$  center excitations. The  $\text{Ag}_3^+$  subunit is created after insertion of one Ag atom of  $\text{Ag}_4$  into the SH bond of the cysteine residue. Such strong localized absorption is typical for silver hybrids and is not present in gold hybrids since there the d-electrons dominate the excitations giving rise to a number of low intensity transitions spread over a broad energy range. In summary, the presented findings indicate that

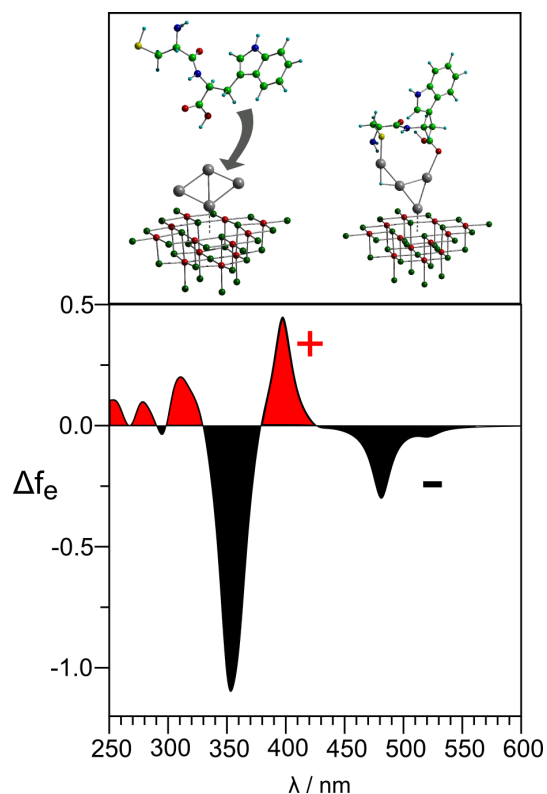


**Fig. 6** Optical signal generated upon binding of a bare Cys-Trp dipeptide to a supported  $\text{Ag}_4$  cluster given by difference of spectra of supported  $\text{Ag}_4$ -CysTrp and bare supported  $\text{Ag}_4$  as indicated by the scheme in the upper panel. A "+" (red areas) indicates an increase of absorption intensity, "-" (black areas) a decrease of absorption intensity.

supported silver cluster hybrid systems can be suitable building blocks for development of biosensing materials.

## 5 Acknowledgement

We acknowledge long term stimulating and fruitful cooperation with L. Wöste and his team. Financial support by the Deutsche Forschungsgemeinschaft priority program SPP 1153 "Clusters at Surfaces: Electron Structure and Magnetism" is gratefully acknowledged. A. K. and R. M. acknowledges the financial support in the framework of the "Emmy-Noether-Programme" (ENP-MI-1236) of the Deutsche Forschungsgemeinschaft (DFG).

## References

- 1 E. Katz and I. Willner, *Angew. Chem. Int. Ed.*, 2004, **43**, 6042–6108.
- 2 M. E. Stewart, C. R. Anderton, L. B. Thompson, J. Maria, S. K. Gray, J. A. Rogers and R. G. Nuzzo, *Chem. Rev.*, 2008, **108**, 494–521.
- 3 R. Wilson, *Chem. Soc. Rev.*, 2008, **37**, 2028–2045.

- 
- 4 R. E. Palmer and C. Leung, *Trends Biotechnol.*, 2007, **25**, 48 – 55.
  - 5 J. R. Lakowicz, *Anal. Biochem.*, 2005, **337**, 171–194.
  - 6 L. Zhao, L. Jensen and G. Schatz, *J. Am. Chem. Soc.*, 2006, **128**, 2911–2919.
  - 7 A. N. Kapanidis and S. Weiss, *J. Chem. Phys.*, 2002, **117**, 10953–10964.
  - 8 R. Ando, H. Mizuno and A. Miyawaki, *Science*, 2004, **306**, 1370–1373.
  - 9 J. R. Lakowicz, *Plasmonics*, 2006, **1**, 5–33.
  - 10 E. G. Matveeva, T. Shtoyko, I. Gryczynski, I. Akopova and Z. Gryczynski, *Chem. Phys. Lett.*, 2008, **454**, 85–90.
  - 11 N. Nath and A. Chilkoti, *J. Fluoresc.*, 2004, **14**, 377–389.
  - 12 I. Gryczynski, J. Malicka, Z. Gryczynski and J. R. Lakowicz, *J. Phys. Chem. B*, 2004, **108**, 12568–12574.
  - 13 J. R. Lakowicz, J. Malicka, I. Gryczynski and Z. Gryczynski, *Biochem. Biophys. Res. Commun.*, 2003, **307**, 435 – 439.
  - 14 M. A. El-Sayed, *Acc. Chem. Res.*, 2001, **34**, 257–264.
  - 15 K.-S. Lee and M. A. El-Sayed, *J. Phys. Chem. B*, 2006, **110**, 19220–19225.
  - 16 E. Cottancin, G. Celep, J. Lerme, M. Pellarin, J. R. Huntzinger, J. L. Vialle and M. Broyer, *Theor. Chem. Acc.*, 2006, **116**, 514–523.
  - 17 J. Yu, S. A. Patel and R. M. Dickson, *Angew. Chem. Int. Ed.*, 2007, **46**, 2028–2030.
  - 18 J. Yu, S. Choi and R. M. Dickson, *Angew. Chem. Int. Ed.*, 2009, **48**, 318–320.
  - 19 Y. Antoku, J. ichi Hotta, H. Mizuno, R. M. Dickson, J. Hofkens and T. Vosch, *Photochem. Photobiol. Sci.*, 2010, **9**, 716–721.
  - 20 V. Bonačić-Koutecký, V. Veyret and R. Mitrić, *J. Chem. Phys.*, 2001, **115**, 10450–10460.
  - 21 C. Sieber, J. Buttet, W. Harbich, C. Félix, R. Mitrić and V. Bonačić Koutecký, *Phys. Rev. A*, 2004, **70**, 041201.
  - 22 P. Radcliffe, A. Przystawik, T. Diederich, T. Döppner, J. Tiggesbäumker and K.-H. Meiwes-Broer, *Phys. Rev. Lett.*, 2004, **92**, 173403.
  - 23 J. Zheng, P. R. Nicovich and R. M. Dickson, *Annu. Rev. Phys. Chem.*, 2007, **58**, 409–431.
  - 24 T. Tabarin, A. Kulesza, R. Antoine, R. Mitrić, M. Broyer, P. Dugourd and V. Bonačić Koutecký, *Phys. Rev. Lett.*, 2008, **101**, 213001.
  - 25 K. Kneipp, H. Kneipp, I. Itzkan, R. R. Dasari and M. S. Feld, *Chem. Phys.*, 1999, **247**, 155 – 162.
  - 26 T. G. Schaaff and R. L. Whetten, *J. Phys. Chem. B*, 2000, **104**, 2630.
  - 27 J. Zheng, J. T. Petty and R. M. Dickson, *J. Am. Chem. Soc.*, 2003, **125**, 7780.
  - 28 J. Zheng, P. R. Nicovich and R. M. Dickson, *Annu. Rev. Phys. Chem.*, 2007, **58**, 409.
  - 29 A. Kulesza, R. Mitrić and V. Bonačić-Koutecký, *Chemical Physics Letters*, 2011, **501**, 211 – 214.
  - 30 I. Compagnon, T. Tabarin, R. Antoine, M. Broyer, P. Dugourd, R. Mitrić, J. Petersen and V. Bonačić-Koutecký, *J. Chem. Phys.*, 2006, **125**, 164326.
  - 31 C. Bürgel, R. Mitrić and V. Bonačić-Koutecký, *Physica Status solidi (B)*, 2010, **247**, 1099–1108.
  - 32 D. Andrae, U. Haeussermann, M. Dolg, H. Stoll and H. Preuss, *Theor. Chim. Acta*, 1990, **77**, 123.
  - 33 S. Gilb, P. Weis, F. Furche, R. Ahlrichs and M. M. Kappes, *J. Chem. Phys.*, 2002, **116**, 4094–4101.
  - 34 A. D. Becke, *J. Chem. Phys.*, 1993, **98**, 5648.
  - 35 C. Lee, W. Yang and R. G. Parr, *Phys. Rev. B*, 1988, **37**, 785.
  - 36 S. J. Vosko, L. Wilk and M. Nusair, *Can. J. Phys.*, 1980, **58**, 1200.
  - 37 P. J. Stephens, F. J. Devlin, C. F. Chabalowski and M. J. Frisch, *J. Phys. Chem.*, 1994, **98**, 11623.
  - 38 M. J. S. Dewar, E. G. Zoebisch, E. F. Healy and J. J. P. Stewart, *J. Am. Chem. Soc.*, 1985, **107**, 3902.
  - 39 P. V. Sushko, A. L. Shluger and C. R. Catlow, *Surface Science*, 2000, **450**, 153.
  - 40 P. J. Hay and W. R. Wadt, *J. Chem. Phys.*, 1985, **82**, 284.
  - 41 B. G. Dick and A. W. Overhauser, *Phys. Rev.*, 1958, **112**, 90.
  - 42 A. L. Shluger, A. L. Rohl, D. H. Gay and R. T. Williams, *J. Phys.: Condens. Matter*, 1994, **6**, 1825.
  - 43 J. P. Perdew and Y. Wang, *Physical Review B*, 1992, **45**, 13244–13249.
  - 44 J. P. Perdew, K. Burke and M. Ernzerhof, *Physical Review Letters*, 1996, **77**, 3865–3868.
  - 45 K. Eichkorn, F. Weigend, O. Treutler and R. Ahlrichs, *Theoretical Chemistry Accounts: Theory, Computation, and Modeling (Theoretica Chimica Acta)*, 1997, **97**, 119–124.
  - 46 R. Ahlrichs, M. Bär, M. Häser, H. Horn and C. Kölmel, *Chem. Phys. Lett.*, 1989, **162**, 165.
  - 47 D. Rappoport and F. Furche, *J. Chem. Phys.*, 2005, **122**, 064105.
  - 48 F. Furche and D. Rappoport, in *Density functional theory for excited states: equilibrium structure and electronic spectra*, ed. M. Olivucci, Elsevier, Amsterdam, 2005, vol. 16, ch. III.
  - 49 R. H. Byrd, P. Lu, J. Nocedal and C. Zhu, *SIAM J. Scientific Computing*, 1995, **16**, 1190.
  - 50 G. N. Khairallah and R. A. J. O’Hair, *Dalton Trans.*, 2005, 2702–2712.
  - 51 G. N. Khairallah and R. A. J. O’Hair, *Angewandte Chemie*, 2005, **117**, 738–741.